

Magnetic Moments and Adiabatic Magnetization of Free Cobalt Clusters

Xiaoshan Xu, Shuangye Yin, Ramiro Moro, and Walt A. de Heer

School of Physics, Georgia Institute of Technology, Atlanta, Georgia 30332, USA

(Received 18 February 2005; revised manuscript received 13 June 2005; published 1 December 2005)

Magnetizations and magnetic moments of free cobalt clusters Co_N ($12 < N < 200$) in a cryogenic ($25 \text{ K} \leq T \leq 100 \text{ K}$) molecular beam were determined from Stern-Gerlach deflections. All clusters preferentially deflect in the direction of the increasing field and the average magnetization resembles the Langevin function for all cluster sizes even at low temperatures. We demonstrate in the avoided crossing model that the average magnetization may result from adiabatic processes of rotating and vibrating clusters in the magnetic field and that spin relaxation is not involved. This resolves a long-standing problem in the interpretation of cluster beam deflection experiments with implications for nanomagnetic systems in general.

DOI: [10.1103/PhysRevLett.95.237209](https://doi.org/10.1103/PhysRevLett.95.237209)

PACS numbers: 75.50.Tt, 73.22.-f, 75.75.+a

Why is a ferromagnetic particle attracted to a magnet? The answer is simple for large particles but it is quite subtle for clusters containing only a few atoms. Isolated, ferromagnetic clusters in molecular beams are attracted to the high-field pole of a Stern-Gerlach (SG) magnet [1–6]. This does not happen for single atoms because spatial quantization of the spin S along the magnetic field B (combined with angular momentum conservation) causes discrete magnetization states $m = 2\mu_B S_z$ ($-S \leq S_z \leq S$). Since the force on the atom is $F = mdB/dz$, deflection maxima are symmetric: half of the atoms are attracted (deflect in the $+z$) and half are repelled. This is conveniently visualized in the Zeeman diagram of an atom [Fig. 1(a)]. By definition $m = -dE/dB$, so that states with negative slope deflect toward the high field and vice versa [7]. Since clusters deflect asymmetrically there is a fundamental difference in the way clusters deflect compared with atoms.

The total spin S_N of Co_N is (approximately) $S_N \approx NS_1$ where S_1 is $1\hbar$ and the magnetic moment $\mu_N \approx 2N\mu_B$ [2]. Individual clusters deflect uniquely in the high-field direction so that for each cluster $m > 0$. This means that the spin tends to align with the magnetic field. Strikingly as shown below, the *average* magnetization M_N of a beam of Co_N appears to follow the Langevin function [8,9] $L(x) = M_N/\mu_N = \tanh x - 1/x$, where $x = \mu_N B/kT$, T is the temperature, and B is the field strength. Note that for small x , $L(x) = x/3$; for large x , $L(x) = 1$.

Since the Langevin function results from the thermodynamic equilibrium of a (large) spin in a magnetic field in a heat bath [Fig. 1(a)], suggesting that the spin thermally relaxes while in the magnetic field. This implies thermalizing transitions between magnetic sublevels, Fig. 1(a). The spin-relaxation model for free clusters was previously assumed [3,4,10] in analogy with the well-known superparamagnetic model of supported small ferromagnetic particles [8]. However, for the thermal relaxation process to occur in isolated clusters requires that the heat bath is internal to the cluster. It further implies a relaxation time, τ , which, in order to be effective, must be short compared

with the transit time through the magnet $t_{\text{mag}} \approx 100 \mu\text{s}$. A large, warm cluster may serve as a thermal bath for its own spin, particularly when many vibrational and electronic modes are excited. However, when $T < T_{\text{Debye}}/N^{1/3}$ and $T < T_{\text{Fermi}}/N$ ($T_{\text{Debye}} \approx 450 \text{ K}$ and $T_{\text{Fermi}} \approx 8 \times 10^4 \text{ K}$) [9] then most of the clusters are in their vibrational and electronic ground states [11,12] and this picture should break down. Nevertheless, we experimentally show that Langevin-like behavior is observed for all clusters at all temperatures.

A beam of cold cobalt clusters is produced in a laser vaporization cluster source [11,13] consisting of a cryogenically cooled chamber ($\approx 0.5 \text{ cm}^3$) with an exit nozzle ($\approx 1 \text{ mm}$ diameter). A pulse of cold He gas is injected into the chamber as focused light from a pulsed laser vaporizes a minute amount of cobalt from a cobalt rod in the chamber. The vapor condenses into clusters. The clusters dwell in the chamber for about 1 ms after which the thermalized clusters are ejected into a high vacuum chamber [2,3,11]. The resulting cluster beam is collimated and passes through a SG magnet ($B \leq 2 \text{ T}$, $dB/dz = 0.25B \text{ T/cm}$; magnet length $L_{\text{mag}} = 6 \text{ cm}$) situated 1 m from the source. The clusters then enter a position sensitive time-of-flight (TOF) mass spectrometer [11,13] situated $L_{\text{TOF}} = 1 \text{ m}$ downstream from the magnet which simultaneously measures their deflections d and their masses m . Velocities v are determined using a chopper. The magnetization is determined from $d_N = m_N(dB/dz)L_{\text{mag}}L_{\text{TOF}}/\text{mass}_N v_N^2$.

Hence, the magnetization $m_N(B)$ of every individual cluster is determined. Figure 2 shows the deflections and the magnetization distribution of Co_{20} for $T = 40 \text{ K}$. Notice the broad magnetization distribution: $m_N/N = 0-2\mu_B$. The 3D plot [Fig. 2(b)] of m_N/N for $12 \leq N \leq 200$ at $T = 40 \text{ K}$ for $B = 2.0 \text{ T}$ qualitatively shows Langevin-like behavior ($\mu_N \approx 2N\mu_B$ so that $x \approx 2N\mu_B B/kT$); however, the magnetization distributions are broad and they do not significantly narrow for larger clusters.

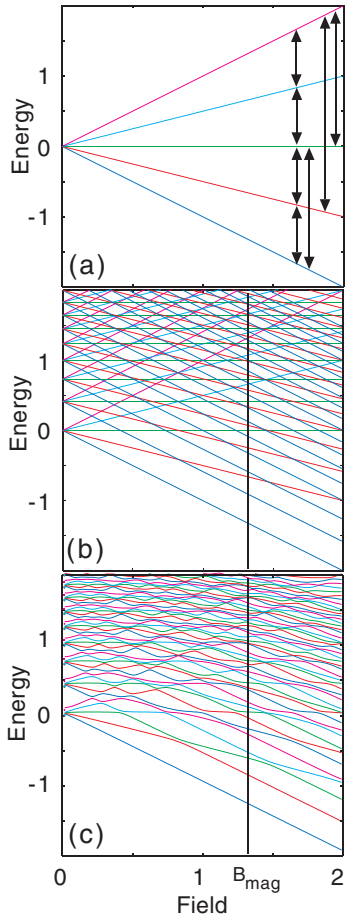


FIG. 1 (color). Schematic Zeeman diagram of a cluster ($S = 2$) for various couplings. (a) Spin 2 cluster coupled to a heat bath causing transitions at a rate ν between the $2S + 1$ Zeeman levels (examples are indicated by arrows). If the transition time $\tau = 1/\nu$ is such that $\tau \gg t_{\text{mag}}$ (the time of passage through the magnet) then the SG deflection pattern consist of $2S + 1$ symmetrically positioned deflection maxima as in the uncoupled case. However, if $\tau \ll t_{\text{mag}}$, the $2S + 1$ maxima collapse in a single deflection maximum in the direction of increasing field [the width of the peak $\Delta M/\mu \approx \sqrt{(\tau/t_{\text{mag}})}$], and peak position follows the Brillouin function (that converges to the Langevin function for large S). (b) Spin coupled to the rotations (all levels in this schematic diagram have the same $J_z = R_z + S_z$). If the spin is uncoupled from the rotations then the deflections are as in (a). (c) Now the spin is coupled to the rotations causing avoided crossings. Note that all of the adiabatic Zeeman levels tend downward with increasing field, indicating increasing magnetization with increasing field causing single-sided deflections. The Zeeman levels are canonically populated in the source (temperature T ; $B = 0$). The levels follow their adiabatic paths into the magnet ($B = B_{\text{mag}}$) and the clusters deflect according to their magnetizations m , i.e., the slope of the levels at B_{mag} (for real clusters, the separation between avoided crossings is so small that the measurement averages over several of them.) The average magnetizations for large S are Langevin-like: for low fields, $M = \mu^2 B/3kT$ ($\mu = 2\mu_B S$) and for large fields $M = \mu$ independent of the density of states. The magnetization distribution width depends primarily on the density of states (see text).

Figure 3 shows that the *average* magnetization M_N is a universal function of x : in Fig. 3(a) M_{100}/μ_{100} is plotted for a wide range of fields and temperatures. Figure 3(b) shows that this trend is followed for all clusters from $N = 20$ to 300. These data show that they fall on a curve, which linearly rises for small x ($M = C_1 x$) and saturates for large x [$M(x \gg 1) = \mu_{\text{sat}}$]; in fact, $C_1/\mu_{\text{sat}} \approx 1/3$ so that for small x , $M_N = \mu_N x/3$ as predicted by the Langevin function. However, the approach to saturation appears to be faster than predicted.

Accordingly, the magnetic moments of cobalt clusters are evaluated from the magnetization data. The magnetic moments per atom μ_N/N [Fig. 3(c)] are enhanced compared with the bulk value ($\mu_{\text{bulk}} = 1.7\mu_B/\text{atom}$ [9]). The enhancement has been attributed to the lower coordination of the surface atoms [2] since the consequent reduced overlap of the majority and minority spin bands enhances the magnetic moment.

Previously the Langevin function was assumed for relatively warm clusters in molecular beams in the small x limit. Here we empirically demonstrated its validity not only in that case but even for small clusters at low temperatures in the small x and the large x limit. This needs to be explained. For supported superparamagnetic particles

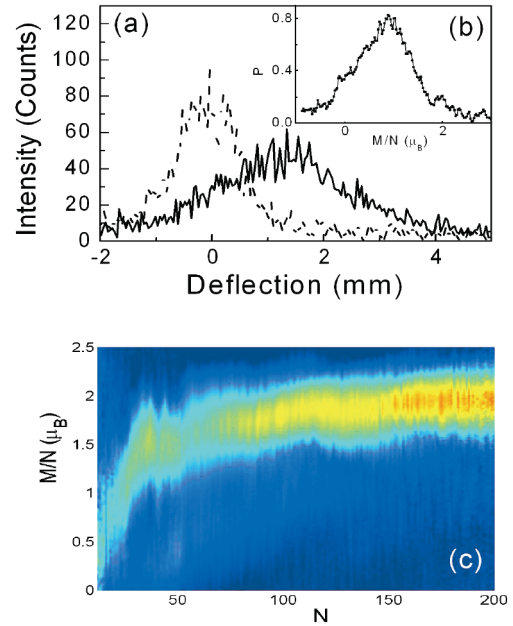


FIG. 2 (color). Deflections and magnetization distributions of Co_N at $T = 40$ K and $B = 2$ T. (a) Position sensitive TOF mass peak of Co_{20} showing the field off (dashed line) and the field on ($B = 2$ T, solid line) deflections (the entire spectrum is composed of about 200 distinct mass peaks). Note the single-sided deflections. (b) (inset) The normalized magnetization probability distribution determined from the deflections in (a) $N = 20$; $M/N = 0.83\mu_B$; $\mu/N = 2.3\mu_B$; $x = 1.5$; $\Delta M/\mu \approx 0.4$. (c) Normalized magnetization distributions of Co_N ($12 \leq N \leq 200$, $T = 40$ K, $B = 2$ T). Amplitudes are represented in color (blue: low; red: high). The magnetization is linear with N for small N and saturates at about $\mu(N) \approx 2N\mu_B$ for large N .

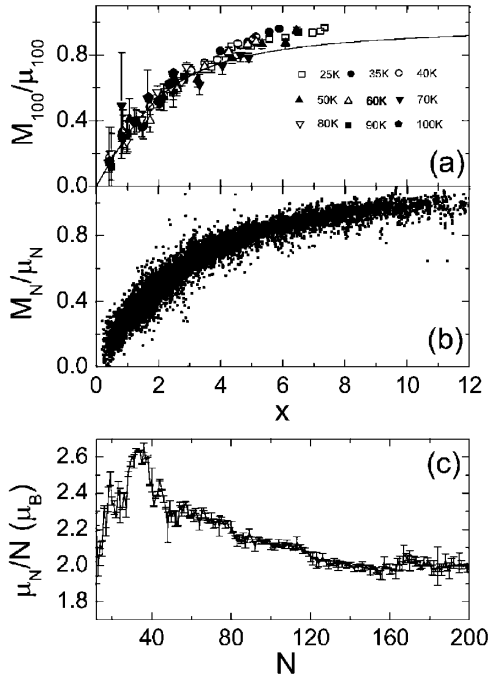


FIG. 3. Magnetic moments μ_N and normalized magnetizations M_N/μ_N of Co_N . (a) M_{100}/μ_{100} of Co_{100} for $25 \text{ K} \leq T \leq 100 \text{ K}$ and $0 < B \leq 2 \text{ T}$, corresponding to x ranging from 0.4 to 12. The data scale with x . Note the linear increase for small x : $M_{100}/\mu_{100} \approx 0.3x$ and $M_{100}/\mu_{100} = 1$ for large x . The trend is consistent with the Langevin function (bold line); however, the Langevin function approaches saturation more slowly. (b) M_N/μ_N for $12 \leq N \leq 200$, $20 \text{ K} \leq T \leq 100 \text{ K}$ and $B \leq 2 \text{ T}$ measured in 63 data sets (9 temperatures from 25 K to 100 K and 7 fields from 0 to 2 T, representing about 10 000 data points), plotted as a function of x . (c) Magnetic moments per atom for Co_N . Note that $\mu_{12}/12 \approx 2\mu_B$, μ_N/N increases to a maximum at $N = 37$ followed by a gradual decrease with weak oscillations converting to $2\mu_B$ for $N = 150$.

the Langevin function results from spin relaxation as indicated in Fig. 1(a) [8]. Does spin relaxation also occur in isolated clusters that are in their vibrational and electronic ground states? First note that if the spin thermally relaxes when the cluster is in the magnet then the width of the magnetization distribution $\Delta M/\mu \approx \sqrt{(\tau/t_{\text{mag}})}$ where $t_{\text{mag}} = L_{\text{mag}}/v \approx 0.09/\sqrt{T}$ s. The observed broad widths indicate that $\tau \approx t_{\text{mag}}$. However, $\Delta M/\mu$ does not show the expected sensitivity to t_{mag} (using various magnet lengths, and various beam velocities) nor does $\Delta M/\mu$ vary signif-

icantly with T or with N . Hence $\sqrt{(\tau/t_{\text{mag}})}$ cannot account for the widths. Consequently, thermal relaxation involving transitions between Zeeman levels [Fig. 1(a)] cannot explain this observation. The origin of the Langevin-like behavior should be sought elsewhere.

We next show that Langevin-like behavior can be naturally explained without invoking spin relaxation by considering the consequences of an interaction of the spin with rotations. The following abbreviated discussion of the avoided crossing model illustrates the principles [14]. Consider the restricted Zeeman diagram of a spin S cluster in Fig. 1(b) which schematically depicts the Zeeman levels of the lowest rotational states with the same (i.e., conserved) $J_z = R_z + S_z$ where R is the rotational angular momentum [7,15]. The separation between rotational levels is (on average) $C_0 = \hbar^2/2I$ where I is the moment of inertia [7,15]. If the spin and the rotation are decoupled then the levels cross [Fig. 1(b)]. However, if they are even weakly coupled then in principle all crossings are avoided [7,15]. This has a profound effect on the magnetization since the resulting adiabatic Zeeman levels [Fig. 1(c)] all tend downward with increasing field and their slopes saturate at $m = \mu$ [Fig. 1(c)]. This means that [after averaging, see below and [16]] all levels have positive magnetization which explains the single-sided deflections.

Specifically, consider a cluster that is created in the source ($B = 0$) in a heat bath at temperature T after which it is thermally isolated and then introduced in a magnetic field ($B = B_1$). This cluster occupies a level which it adiabatically follows from $B = 0$ to $B = B_1$. For small B_1 the magnetization vanishes (since the average slope vanishes) while for large B_1 it saturates at $M = \mu$ (the slope tends to $-\mu$). This explains in principle how the spin-rotation coupling causes deflections in the high-field direction without invoking spin relaxation. This process is adiabatic and does not involve a relaxation time nor coupling to a heat bath. Note that similar adiabatic deflection processes have been previously proposed for specific cases [17–19].

The average magnetization for weak fields is obtained with little effort. Consider the point $E(B)$ in the Zeeman diagram [Fig. 1(b)]. In the uncoupled Zeeman diagram $E_{\text{uc}}(B) = E_{\text{uc}}(0) - mB$ ($\mu = 2\mu_B S$; $M = 2\mu_B S_z$; $-S \leq S_z \leq S$). In the coupled Zeeman diagram all crossings are avoided [Fig. 1(c)]. The slope at $E(B)$ in the coupled diagram equals the average of all the slopes of levels passing through $E_{\text{uc}}(B)$ in the uncoupled diagram [20]. Hence, for large S

$$-\langle dE/dB \rangle = m(E, B) = \int_{-\mu}^{\mu} m\rho(E + mB)dm / \int_{-\mu}^{\mu} \rho(E + mB)dm, \quad m(E, B \rightarrow 0) = \frac{\mu^2 B}{3\rho(E)} \frac{\partial \rho(E)}{\partial E}, \quad (1)$$

where $\rho(E)$ is the (restricted) density of states at $B = 0$. The average adiabatic magnetization M is found by thermally populating the states in zero field and measuring the average magnetization in field B :

$$M(B) = \frac{\int m(E, B)\rho(E)e^{-E/kT}dE}{\int \rho(E)e^{-E/kT}dE} = \frac{\mu^2 B}{3kT} = \frac{\mu x}{3}$$

Note that the average magnetization does not depend on $\rho(E)$. Furthermore, for high fields, $M(B) \rightarrow \mu$. This remarkable result demonstrates that both the average low-field and high-field magnetization follow the Langevin function; however, spin relaxation in the magnet is not required. [For finite S the integral in Eq. (1) is replaced by a sum yielding $M(B) = 2S(S+1)\mu_B^2 B/3kT$: the low-field limit of the Brillouin function.]

Intermediate fields require knowledge of the density of states. Assuming that $\rho(E) \propto E^\gamma$ then numerical calculations show that $M(B)$ rapidly asymptotically approaches the Langevin function as the number of independent occupied modes in the cluster γ is increased (as it will with increasing cluster size). The widths of the distributions $\Delta M/\mu$ qualitatively correspond with observations. For example, for $\gamma = 1$, $\Delta M/\mu \approx 0.4$ for $x = 0.5$ to 5 . Hence the rather large observed widths are also explained.

The coupled Zeeman diagram discussed here is a special case of the energy level spectrum of irregular systems discussed by Berry [21] and Pechukas [22], where level repulsions cause energy levels with approximately the same energy to have approximately the same slope. The ferromagnetic clusters studied in this Letter are examples of irregular systems where couplings cause energy levels to become approximately parallel.

We next address an important detail: if the gap at an avoided crossing is very small then there is a finite probability that the gap is “jumped” (i.e., the gap is ignored) in the measurement. The nonadiabatic transition probability is given by the Landau-Zener [23] equation:

$$p = \exp\left(-\frac{\pi\Delta^2}{2g_B|m - m'|dB/dt}\right),$$

where p is the probability for a nonadiabatic transition, m and m' are the magnetizations of the intersecting Zeeman levels, and dB/dt is the rate of change of the magnetic field in the deflection field: in our experiments $dB/dt < 2$ T/s. Hence, $p = 0$ for a gap with $\Delta \gg 10^{-8}$ eV, and the crossing is traversed adiabatically; if $\Delta \ll 10^{-8}$ eV, $p = 1$ and the gap is traversed nonadiabatically; if $\Delta \approx 10^{-8}$ eV, the probability p is significantly removed from those extremes causing irreversible behavior. It can be shown that if the gap sizes are random then our conclusions still hold. Significant deviations only occur when $\Delta \ll 10^{-8}$ eV for essentially all of the gaps, in which case the spin is effectively uncoupled. In that case, spin alignment does not occur.

We have experimentally demonstrated that the Langevin-like average magnetization of ferromagnetic cluster beams is a property of the ensemble of isolated clusters in the beam, not of the individual clusters.

This phenomenon may be more general: it may supplement superparamagnetic relaxation (which involves a relaxation time) in supported ferromagnetic clusters especially when the coupling to the support is weak. In that case the rotations are replaced with soft vibrational and tor-

sional modes of the cluster on its support, and should produce a Langevin-like adiabatic response. Furthermore, the magnetization changes at avoided crossing (substituting the rotations with oscillations in the anisotropy wells) may be an alternative way to represent the magnetization transitions in magnetic molecules that are often viewed as a tunneling process between magnetic states of the molecule.

-
- [1] W. A. de Heer *et al.*, Phys. Rev. Lett. **65**, 488 (1990).
 - [2] I. M. L. Billas *et al.*, Science **265**, 1682 (1994).
 - [3] J. P. Bucher *et al.*, Phys. Rev. Lett. **66**, 3052 (1991).
 - [4] D. C. Douglass *et al.*, Phys. Rev. B **47**, 12 874 (1993).
 - [5] T. Hihara *et al.*, Chem. Phys. Lett. **294**, 357 (1998); S. Pokrant, Phys. Rev. A **62**, 051201 (2000).
 - [6] M. B. Knickelbein, Phys. Rev. Lett. **86**, 5255 (2001).
 - [7] C. H. Townes and Schawlow, *Microwave Spectroscopy* (Dover, New York, 1955).
 - [8] C. P. Bean and J. D. Livingston, J. Appl. Phys. **30**, 120S (1959).
 - [9] C. Kittel *Introduction to Solid State Physics* (Wiley, New York, 1996), 7th ed.
 - [10] S. N. Khanna and S. Linderoth, Phys. Rev. Lett. **67**, 742 (1991).
 - [11] W. A. de Heer, Rev. Mod. Phys. **65**, 611 (1993).
 - [12] For Co_N , the low frequency cutoff in the vibrational spectrum $\omega_{\min} \approx \omega_{\text{Debye}}/N^{1/3}$ where $T_{\text{Debye}} \approx 450$ K. The fraction of cobalt clusters occupying the vibrational ground state is $P(N, T) \approx \prod [1 - \exp(-\hbar\omega_i/kT)]$ where ω_i are the $3N - 6$ vibrational modes: $\omega_{\min} \leq \omega \leq \omega_{\text{Debye}}$. For $T \leq 20$ K, more than half of the clusters with $N < 200$ (and essentially all cluster with $N < 50$) are in the vibrational ground state.
 - [13] R. Moro *et al.*, Science **300**, 1265 (2003).
 - [14] W. A. de Heer Ph.D. thesis, University of California, Berkeley, 1985.
 - [15] J. H. van Vleck, Rev. Mod. Phys. **23**, 213 (1951).
 - [16] The separation between crossings on a level is $\Delta B \approx C_0/\mu \approx 0.1 \text{ N}^{-8/3} \text{ T}$ (i.e., 10^{-4} T for $N = 10$), which is much smaller than the field resolution of the magnet.
 - [17] N. A. Kuebler *et al.*, Phys. Rev. A **38**, 737 (1988).
 - [18] P. Ballone *et al.*, Phys. Rev. B **44**, 10 350 (1991).
 - [19] G. F. Bertsch and K. Yabana, Phys. Rev. A **49**, 1930 (1994); V. Visuthikraisee and G. F. Bertsch, Phys. Rev. A **54**, 5104 (1996); N. Hamamoto *et al.*, Phys. Rev. B **61**, 1336 (2000).
 - [20] Consider a point $E(B)$ in the Zeeman diagram in the limit of vanishing coupling. All the Zeeman levels that pass through this point originate from the 0 field energy $E(0) = E(B) - M_Z B$; the slope of each of those levels is $M_Z = g\mu_B S_Z$. The average slope of the adiabatic energy level through $E(B)$ is the found by summing the slopes after weighting them with their appropriate densities of states at $B = 0$ (this is easy to demonstrate diagrammatically).
 - [21] M. V. Berry and M. Tabor, Proc. R. Soc. Lond., Ser. A **356**, 375 (1977).
 - [22] P. Pechukas, Phys. Rev. Lett. **51**, 943 (1983).
 - [23] C. Zener, Proc. Roy. Soc. **137**, 833 (1932).